Nitrous Oxide as a Substitute for Sulfur Hexafluoride in the ANSI/ASHRAE 110 Method of Hood Performance Evaluation
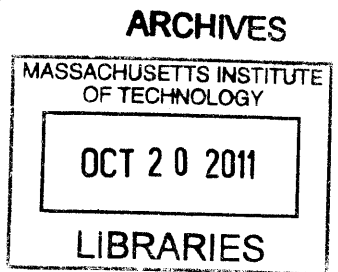
by

Eric J. Guffey

Submitted to the Department of Mechanical Engineering in Partial
Fulfillment of the Requirements for the Degree of

Bachelor of Science in Mechanical Engineering
at the
MASSACHUSETTS INSTITUTE OF TECHNOLOGY

January 2011
© 2011 Eric J. Guffey
All rights reserved

The author hereby grants to MIT permission to reproduce and to
distribute publicly paper and electronic copies of this thesis document in whole or in part
in any medium now known or hereafter created.

Signature of Author..
Department of Mechanical Engineering
January 14, 2011

Certified by ....
Professor Leslie Norford
Professor of Building Technology
Thesis Supervisor

Accepted by ....
Professor John H. Lienhard V
Chairman, Undergraduate Thesis Committee

1

Nitrous Oxide as a Substitute for Sulfur Hexafluoride in the ANSI/ASHRAE 110 Method of Hood Performance Evaluation

by

Eric J. Guffey

ABSTRACT:

The ANSI/ASHRAE 110 Method is the standard test for laboratory hood containment performance. Sulfur hexafluoride is specified as the gas most suitable for this test and is most commonly used. Sulfur hexafluoride use has potential negative environmental repercussions as it is a potent greenhouse gas with a global warming potential 22,800 times greater per mass than CO_2. The purpose of this study is to evaluate nitrous oxide, a much less environmentally destructive tracer gas, as a potential substitute in the ANSI/ASHRAE 110 Method.

In accordance with ANSI standards, flow visualization, face velocity, and tracer gas tests were performed on numerous laboratory hoods of varying design. A mannequin was positioned in front of the center of the hood, and a MIRAN SapphIRe was used to measure the presence of each tracer gas. Direct comparisons of the concentrations of the two gases were dominated by a few high concentrations. For this reason, concentrations of both gases were log10-transformed for statistical analyses.

Laboratory hood dimensions and properties were found to affect the relationship between the gases. The hood area of opening and sash height were found to significantly ($p<0.001$) affect $\log_{10}(SF_6/N_2O)$. Average face velocity also significantly ($p<0.025$) affected the log ratio. Neither gas was an adequate indicator of the behavior of the other. The linear best fit of the logs of the concentration ratio had a slope of 0.858, a y-intercept of 0.434, and an R^2 of 35.9% indicating a poor correlation. For N_2O to qualify as a substitute for SF_6 there would need to be a strong correlation between gas concentrations that was consistent independently of hood conditions. This condition was not met. Nitrous oxide was found to not be a suitable substitute for sulfur hexafluoride in the ANSI/ASHRAE 110 Method.

Thesis Advisor: Leslie Norford
Title: Professor of Building Technology

ACKNOWLEDGEMENTS

TABLE OF CONTENTS

LIST OF FIGURES

LIST OF TABLES

INTRODUCTION

Laboratory hoods are widely used to reduce exposure to contaminants and contain hazardous gases in enclosed environments. These hoods are designed to safeguard operators handling hazardous airborne materials. They typically have five completely contained sides and a sixth working side. Exposure directly to the user is partially blocked by a sliding transparent shield known as a sash. Users stand facing the working side and reach under or around the sash to handle objects inside the hood. These sashes are easily adjusted by the user and can be found in a horizontal or vertical configuration. All of the hoods tested in this study had vertical sashes.

ANSI/ASHRAE 110 is a widely accepted standard that specifies a protocol for testing the effectiveness of laboratory hoods in containing contaminants. Sulfur hexafluoride (SF_6) is the tracer gas of that protocol. It is deemed an excellent choice for the procedures due to its density, stability, and ease of detection using infrared absorption.

A major disadvantage in the use of SF_6 is its potential to harm the environment. SF_6 is the most potent greenhouse gas that has been evaluated by the Intergovernmental Panel on Climate Change (2007). They found that it had a global warming potential 22,800 times that of CO_2 for the same mass. This is much higher than other tracer gases that could be used with the ASHRAE protocol, including nitrous oxide (N_2O). The latter has a warming potential of only 298 times that of CO_2.

PURPOSE OF THE STUDY

This study will examine the use of N_2O as a substitute for SF_6 in testing effectiveness of laboratory hood. Nitrous oxide is a commonly used gas in pharmaceutical fields. Its behavior in fume hoods is less studied than SF_6. Replacing SF_6 with N_2O would dramatically reduce the environmental impact of future tracer gas hood studies. However, before any substitution can be made, it is essential that it be shown to be equivalent in testing lab hoods to SF_6.

BACKGROUND

Effectiveness Testing

Success of a fume hood is measured by its ability to limit exposure to the user. Mannequin exposure to tracer gases released inside the hood enclosure is commonly used to predict the propensity of a fume hood to leak gases. In these tests, tracer gases are released from a source at a controlled rate and measured from a fixed, consistent position outside the hood. In ASHRAE 110, that location is the breathing zone of a mannequin simulating an operator at work in front of the hood. Many gases can be chosen for these test procedures. Any gas that escapes the hood is typically measured as a low concentration. The gas selected must normally be present in very low supply in ambient conditions to allow for the detection apparatus to easily distinguish between leaked and normal levels of the substance. Good choices for tracer gases are also inert, non-toxic, colorless, and odorless.

ASHRAE 110 Method

In the U.S., ANSI/ASHRAE 110 (1995) provides guidelines for sash positioning, minimum exhaust air flow, and effectiveness testing using tracer gases. The method consists of face velocity measurements, flow visualization, and a tracer gas test. The tracer gas leak test in ASHRAE 110 is intended for hoods that rely on face velocity to maintain containment (which excludes glove boxes and other totally enclosed hoods).

The ASHRAE 110 method requires that the mannequin be placed with its nose 75 mm from the sash opening and that the tracer gas diffuser be positioned at least 150 mm behind the plane of the sash. According to the ANSI standard, the acceptable level of SF_6 is 0.1 PPM for five minute averages taken at a mannequin's breathing zone. The protocol requires that the 5 minute period start just as the tracer gas is first turned on, which means that the sampling device will be measuring clean air until contaminated air escapes from the hood and reaches the sensor. The standard also specifies the design and placement of the tracer gas sources and the design and placement of the mannequin (see Apparatus).

N_2O Qualification as Replacement for SF_6

Due to the density disparity (6.164 g/L for SF_6 and 1.977 g/L for N_2O), the two gases have the potential to behave significantly differently under identical conditions. Furthermore, sampling instruments may have different accuracy ranges for the two gases.

To serve as an acceptable replacement, N_2O must behave similarly to SF_6 under the same conditions. To qualify as an ideal replacement, N_2O would need to perform identically to SF_6 in

all testing conditions. A direct, proportional response would be highly convenient, but any relationship that can be modeled to predict the behavior of the other gas may be acceptable if it is consistent and precise enough to provide the same results as SF_6 in a test of any hood under any reasonable set of conditions.

The relationship between both gases must be predictable in any hood regardless of dimension and flow characteristics. It is important to note that it is not sufficient that average or median values be equivalent since hoods are rated on the basis of a single test. It is also very important that the variance in results under the same conditions for N_2O be no higher than that of SF_6 so that the specificity of the test is not reduced.
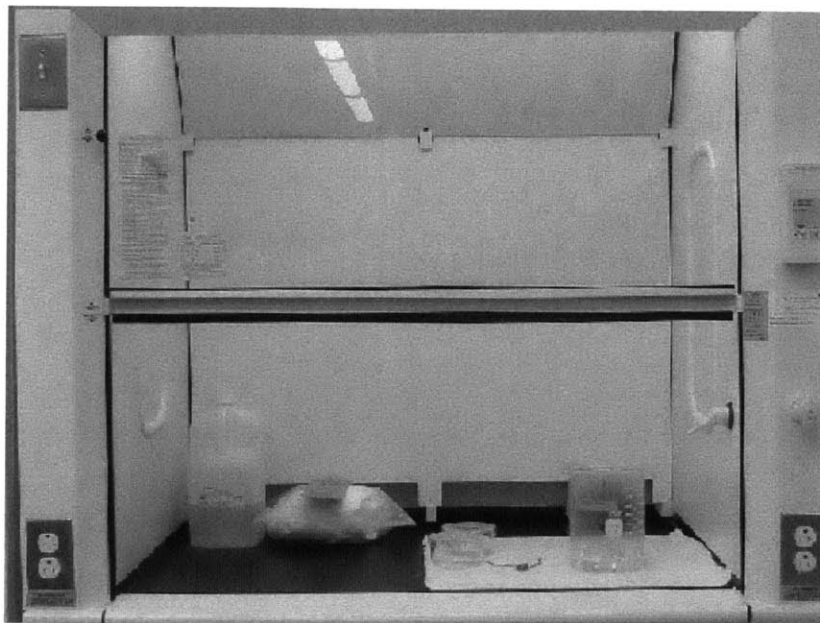
Figure 1: Typical Laboratory Fume Hood

REVIEW OF PUBLISHED LITERATURE

Other studies were examined to understand the factors that affect hood test results. The relevance of factors not investigated here but present in other studies is considered.

Leakage Based on Position

The flow pattern of the controlled gases may play a large role in the ability of a laboratory hood to successfully contain leakage. This pattern is often complex and dependent on many factors, including air flow rate and experimental configuration. Introduction of an obstruction such as a mannequin in front of the hood creates wake zones in the flow and affects rates of leakage (Karaismail and Celik, 2010). Objects within the hood working area may also disrupt flows. Single source points of contaminant specified in ASHRAE 110 may not resemble the most common laboratory source locations. It is likely that in many cases a single source of gas is dispersed over a volume much smaller than the volume of the hood, making it unlikely the gas leakage is distributed evenly throughout the hood face.

Tseng *et al.* (2006) performed tracer gas tests of lab hoods using sulfur hexafluoride, a MIRAN SapphIRe, and diffusers specified by ASHRAE 110. Measurements of SF_6 concentrations were collected over twelve grids on the fume hood with and without a mannequin present. The tracer gas was released 35 cm above the working height of the hood and the detection sensor was placed in the plane of the sash. The tests were performed with the sash opened to heights of 60 cm and 85 cm. The grid areas were distributed so that three formed a vertical line along either side of the outermost horizontal walls of the hood face. Three grid areas traced the outline of the mannequin on either side. The uppermost were at the height of the breathing zone 55 cm above the work height, the middle ones were at chest level, and the lowest were 5 cm above the working height. The measurements for the condition of no mannequin present can be found in Table 1. U denotes upper, M denotes middle, L denotes lowest, the subscript E refers to the edge along the left of right side of the hood opening, and the subscript M refers to the measurements along the outline of the mannequin. The test procedure was repeated with the addition of a mannequin.-Results are shown in Table 2, which was adapted from Tseng *et al.* (2006).

Table 1: Plot of Concentration at Each Position with No Mannequin Present

Cell Position	Mean CSF$_6$ at H = 60 cm (ppb)	Mean CSF$_6$ at H = 85 cm (ppb)
U$_{EL}$	40	80
U$_{ML}$	20	30
U$_{MR}$	20	30
U$_{ER}$	30	80
M$_{EL}$	1300	3780
M$_{ML}$	10	20
M$_{MR}$	20	30
M$_{ER}$	1140	3050
L$_{EL}$	1140	2300
L$_{ML}$	260	1460
L$_{MR}$	390	2070
L$_{ER}$	1880	2490

Table 2: Plot of Concentration at Each Position with Mannequin Present

Cell Position	Mean CSF$_6$ at H = 60 cm (ppb)	Mean CSF$_6$ at H = 85 cm (ppb)
U$_{EL}$	260	140
U$_{ML}$	20	40
U$_{MR}$	40	30
U$_{ER}$	1630	2850
M$_{EL}$	16700	27680
M$_{ML}$	10	50
M$_{MR}$	10	70
M$_{ER}$	22420	38730
L$_{EL}$	24650	37960
L$_{ML}$	5760	12140
L$_{MR}$	22140	37650
L$_{ER}$	77650	66480

The study found that SF$_6$ leakage increased significantly (roughly doubled overall) in nearly every position both when the sash was raised and when the mannequin was added. The mannequin increased concentrations roughly 15 times overall. Clearly the sash height is important but the presence of the mannequin is critical.

The lowest velocity zone consistently had the highest average concentration. One would expect that as the sash height is raised, containment leakage would increase the most in the uppermost regions. In the case with no mannequin, the average middle value increases the most (179%), and the upper increases the least (100%). This suggests that the distribution of the velocities and the exact positioning of the mannequin may be important variables affecting concentrations at the mannequin's breathing zone.

Face Velocity

Face velocity has long been employed as a surrogate for hood effectiveness; however, comparisons to results of tracer gas studies generally have shown poor correspondence between the ASHRAE 110 compliant testing results and hood face velocities. For example, Maupins and Hitchings (1998) performed 178 compliant tracer gas tests at 10 facilities. They found a coefficient of correlation of only 26% between mean face velocity and hood failure as defined by the ANSI standard. They noted that their earlier testing found that while 46% of their hoods met the face velocity requirements, only 13% passed the containment requirements. The lack of correlation, however, could be attributable to the very high variability commonly found in both lab hood ASHRAE 110 testing and face velocity measurements.

Presence and Heating of a Mannequin

As discussed earlier, Teng *et al.* (2006) found that the presence of a mannequin was profoundly important. This agrees with Barnea and Guffey (1994) who found that a mannequin positioned at the face of the hood dramatically increased concentrations outside the hood. Karaismail and Celik (2010) found that the mannequin enhances flow convergence but also induces oscillatory disturbances in the flow that vary with exhaust airflow rate.

Caplan and Knutson (1982) referred to unpublished findings showing very strong effects of a mannequin on the results of what is now the ASHAE 110 test. Although there was a difference when using different sized human test subjects, the difference was much smaller than the change between substituting any sized human for a mannequin.

The difference Caplan and Knutson found between mannequins and humans may be attributable to using an unheated mannequin. The ASHRAE 110 test, which closely follows the methods of Caplan and Knutson (1982), specifies an unheated mannequin. The lack of heating may render the mannequin unrepresentative of workers since body heat induces strong updrafts (Gao and Niu, 2005; Ahn *et al.*, 2008), potentially increasing transport up from the sash bottom to the mannequin's head (Li, *et al.*, 2007).

In a computational fluid dynamics study, Li *et al.* (2005) found that the concentration at the breathing zone varied substantially with the use of different shaped bodies outside the hood. This indicates that hood operator size and posture may play a role in leakage to the breathing zone. Another study found that the placement of arms under the hood and hand movement inside affected tracer gas test results (Ahn, *et al.*, 2008).

Summary

Based on Teng *et al.* (2006) and Maupins and Hitchings (1998), one would expect sash position and face velocity each to affect leakage rates but neither to prove statistically significant. The ASHRAE 110 test may be a poor indicator of a hood's ability to limit exposure to a human operator. Significant leakage has been observed outside of the location specified by the test guidelines (Tseng et al., 2006). Additionally, unheated mannequins may be unrepresentative of human operators due to the effect of body heat and differences in body shape and size (Gao and Niu, 2005; Ahn *et al.*, 2008; Li *et al.*, 2005). However, since this study will not include human subjects, it will not be able to confirm the difference between human and unheated mannequin operators.

13

APPARATUS

Each hood examined in this paper was subjected to three tests (smoke, face velocity, and tracer gas test) to examine their containment effectiveness. Results for each test are described separately.

Smoke Test

A functional fume hood must sufficiently limit exposure at every point under its sash. As required by the ASHRAE 110 method, a smoke test was performed on every hood. The smoke source, a titanium tetrachloride stick, was traced along the outermost perimeter of the hood face. Smoke flow patterns and containment were observed; the results were determined on a pass-fail basis.

Figure 2: Velocicalc Plus Thermo-Anemometer

Face Velocity Test

All hoods tested in this study used face velocity as the primary method of containment, and 24 out of 29 of them were low-flow Thermo Fisher "Concept" hoods. As a result, face velocity was predicted to play a large role in the performance of the hood. Face velocity was measured thoroughly at each hood using a Velocicalc Plus thermo-anemometer (pictured in Figure 2) configured to have a 5 second sampling period for each point. The thermo-anemometer was fixed to a microphone stand to prevent motion through use by human. The anemometer was positioned so that the point of its wand was pointing perpendicular to the direction of the face velocity and directly in the plane of the sash. The sash of the hood was opened fully during these tests. The velocity readings were taken at many points along the face.

The face area was divided into equal size grids, each with dimensions less than or equal to 300 mm, dependent on hood dimensions as shown in Table 3. Face velocity measurements were

made in the center of each grid. Individual grid measurements were kept and analyzed separately. The minimum, maximum, average, and standard deviation of these measurements were calculated and used for further data analysis.

Table 3: Sample Measurement Grids

Hoods Dimensions		Equal Cells in Grid	
Height, mm	Width, mm	No. Rows	No. Columns
450	900	2	3
690	1100	3	4

Tracer Gas Test

An unheated, armless mannequin meeting ANSI requirements for size was used while clothed in a lab coat. The mannequin was positioned with its breathing zone 75 mm from the plane of the sash as seen in Figures 3 and 4. A supporting metal rod was used to keep the mannequin stable and elevated to the correct height. Gas concentration measurements were taken at the mannequin's breathing zone.

A MIRAN SapphIRe was used in the tracer gas test for detection and analysis of both SF_6 and N_2O. Flexible tubing was used to extend the wand of the MIRAN to the breathing zone of the mannequin. Tests using SF_6 and N_2O were performed separately using a release rate of 4 LPM. In compliance with ASHRAE 110, the diffuser for the tracer gas was centered in the hood 150 mm behind the sash. Both the diffuser and supply cylinder were placed inside the hood during SF_6 testing, while only the diffuser was inside the hood during N_2O testing due to size limitations of the supply cylinder.
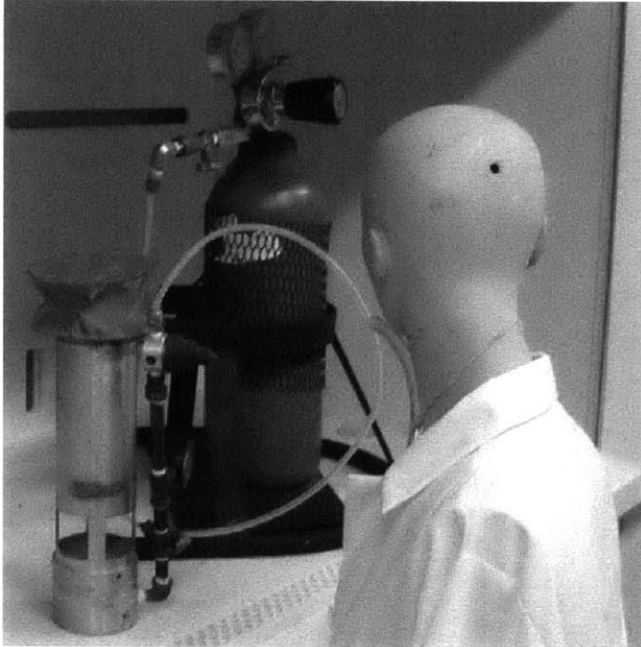
| Figure 3: Cylinder and Diffuser | Figure 4: Positioning of Mannequin |
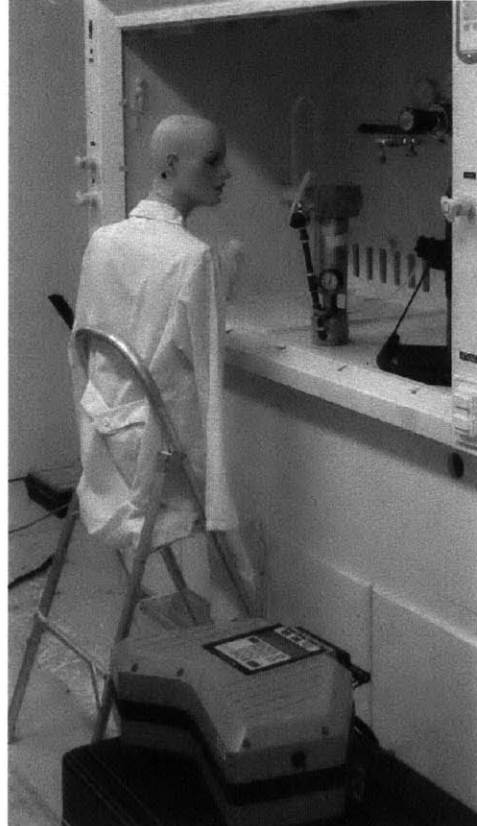
Tracer Gas Measurement Instrument

Gas concentration levels were sensed and recorded using a MIRAN SapphIRe, portable infrared spectrophotometer (see Figure 5). Thermo Fisher Scientific state that they have demonstrated that "The MIRAN SapphIRe meets all criteria set down by NIOSH for performing nitrous oxide tests" identified in NIOSH Method 6600.

A spectrophotometer measures the level of light intensity received after passing a beam of infrared light through a gas mixture. Light intensity measured by the MIRAN is determined by data obtained between wavelengths from 2.5 to 14 micrometers. The level of intensity is dependent on the path length, concentration, and gas specific constant. It obeys Beer's law below in Equation 1.1 (CMB Control, 2010):

$$log\left(\frac{I_0}{I}\right) = kbC \quad\text{..} \quad (1.1)$$

I = light intensity, I_0 = reference light intensity, k = gas specific constant, b = path length, and C = concentration

$$\text{Hence, ideally:} \quad C = \left(\frac{1}{kb}\right) log\left(\frac{I_0}{I}\right) \quad\text{.....................................} \quad (1.2)$$

16

Because of non-linearity's and imperfections, Equation 1.2 actually fits only a small range of concentrations. To extend the range of accurate predictions, Equation 1.2 is expanded to include a quadratic term and corrective multiplier to fit known concentrations and the instrument's response to them by linear regression:

$$C = const_1\left(\left(\frac{1}{kb}\right)log\left(\frac{I_0}{I}\right)\right) + const_2\left(\left(\frac{1}{kb}\right)log\left(\frac{I_0}{I}\right)\right)^2 \quad \text{.............. (1.3)}$$

Using the equation for absorbance: $\quad A = log\left(\frac{I_0}{I}\right) \quad$ .... (1.4)

Equation 1.3 also can be written as:

$$C = const_1\left(\frac{A}{kb}\right) + const_2(\frac{A}{kb})^2 \quad \text{............................ (1.5)}$$

As implied by Equation 1.3, better predictions can be made by calibrating with the assumption that the instrument response is non-linear in the ranges of interest. At still higher levels of a gas, the sensor responds increasingly less to additional amounts of absorbance at an accelerating rate, limiting the range that can be accurately fit using Equations 1.3 or 1.5.

The values of $const_1$ and $const_2$ are specific to each gas and are appropriate for a given sensor only for the wavelength used during the calibration. The use of single wavelength detection can result in false detections of gases if the configured detection wavelengths for both gases overlap. The MIRAN allows the user to adjust the wavelength used to detect each compound. The default wavelength used by the instrument for each gas is optimized to account for sensitivity, maximum range, and interferences with commonly encountered gases (e.g., CO_2, water vapor). The default wavelengths used by the apparatus for the detection of the gases in this study were 4.50 micrometers for N_2O and 10.71 micrometers for SF_6 (Thermo Environmental Instruments, 2010). There was no interference in detection using these wavelengths, so the default wavelengths were employed for both gases.

Figure 5: MIRAN SapphIRe

The ability to accurately determine the concentration present varies among substances. There is both a minimum and a maximum value that can be accurately detected for each gas. From the manufacturer's specifications the detection limit, the point in which the MIRAN can consistently detect the presence of the gas, is 10 ppb and 40 ppb for SF_6 and N_2O, respectively. The range a reading can be considered accurate by the manufacturer extends from five times the detection limit up to the maximum value specified that can be fit accurately with Equation 1.5. For nitrous oxide (N_2O), this range is 200 ppb to 100,000 ppb with ±10% accuracy. For sulfur hexafluoride (SF_6), this range is 50 ppb to 4000 ppb with ±10% up to 1000 ppb and ±20% from 1000 to 4000 ppb. The accuracy of values outside this range was not reported by the manufacturer.

Due to instrument design, the sampling chamber of the MIRAN SapphIRe acts as a dilution chamber so that the contained volume being analyzed at any time is a dynamic mixture of air drawn into the instrument. As a result, measurements are based not only on current concentrations but also earlier concentrations. The time for the apparatus's recorded measurements to approach a steady incoming concentration depends on the previous average concentration in the chamber, the exhaust rate, and the mixing efficiency inside the chamber.

For the study, the MIRAN was turned on when no N_2O or SF_6 was being released in the hood and data logging did not begin until the researcher verified that the concentration of the tracer gas in the chamber had fallen to zero. In other words, the chamber was purged with clean air before measurements were taken.

PROCEDURE

The three tests in this study were performed in the order of smoke test, face velocity test, and then tracer gas test. The procedure for each test was as follows:

Smoke Test

1. Place titanium tetrachloride smoke stick inside protective plastic case and seal
2. Set sash position to working sash height
3. Position titanium tetrachloride plastic case inside hood
4. Unseal plastic case to allow smoke to escape into hood
5. Move plastic case along hood face perimeter positioned so that smoke enters hood
6. Observe smoke effects
7. Confirm hood contains smoke adequately and record in lab notebook

Face Velocity Test

1. Extend the sash to the highest position achievable by the hood
2. Measure the width and the "full open" configuration height
3. Divide hood into equal sized rectangular grids of dimensions less than or equal to 300 mm as shown in Table 3
4. Attach thermo-anemometer to stand
5. Position stand so that anemometer's meter is in the center of the first grid
6. Align anemometer so that its wand is directly in the plane of the sash
7. Rotate anemometer meter radially until perpendicular with plane of sash
8. Step away from apparatus and press "sample"
9. Record individual grid face velocity measurement in lab notebook
10. Repeat steps 5 to 9 for next grid

Tracer Gas Test

1. Verify hood completed smoke test
2. Verify hood completed face velocity test
3. Extend the sash to the highest position achievable by the hood
4. Measure the width and the "full open" configuration height
5. Place the SF_6 dispenser and supply cylinder inside the hood
6. Place dispenser 150 mm behind the plane of the sash centered between the walls
7. Position mannequin, support rod, and elevating stand in front of the hood centered
8. Assemble and Power-on MIRAN SapphIRe
9. Attach extension hose to MIRAN SapphIRe wand, run hose under mannequin lab jacket, and fasten along cheek of mannequin
10. Position mannequin in the center of the hood with the breathing zone 75 mm from the sash
11. Slide sash to 450 mm above working height
12. Allow MIRAN SapphIRe to purge and re-zero data
13. Set MIRAN SapphIRe to begin logging data
14. Observe data to ensure it is consistent around 0 (if not- stop logging data, re-zero, and start recording again)

15. Set supply cylinder gauge at correct pressure to allow a flow of 4 LPM
16. Continue recording data for at least 5 minutes measured from the point of setting the correct pressure
17. Stop logging data
18. Turn off the flow of gas
19. Raise sash height to "full open configuration"
20. Observe data to ensure it is consistent around 0
21. Repeat steps 13 to 18
22. Remove SF_6 dispenser and supply cylinder without disturbing mannequin position
23. Place N_2O dispenser inside the hood
24. Repeat steps 11 to 21
25. Remove N_2O dispenser from hood
26. Record observations into lab notebook

Data Analysis Method

When the MIRAN SapphIRe first began logging data for each test, no gas was being released. Data was monitored to ensure it was consistently around 0 ppb before the gas was turned on. After the measurements displayed were confirmed to be acceptably close to 0 ppb, the control valve on the tracer gas cylinder was opened and the regulator was set at the pressure known to achieve 4 LPM. The amount of time between the initiation of data logging and correctly adjusting the regulator varied due to human input.

Additionally, there was instrument delay in the MIRAN SapphIRe's ability to make measurements consistent with present conditions as discussed in the following section. To eliminate most of the initial period of non-representative sampling, the first minute of logged data was not used in analysis. Instead, the 5 minutes of data logged from minute 1 to minute 6 were used in analyses. The MIRAN SapphIRe sampled at a rate of 2 measurements per second. The average of these 2 measurements was used as the value for that point in time during analysis.

In addition, measurements reported below the detection limit specified by the MIRAN have been adjusted to account for instrument limitations. As recommended by Antweiler and Taylor (2008), logged data below the detection limit was replaced by the value of one-half the detection limit (20 ppb for N_2O and 5 ppb for SF_6).

The raw data results of a previous study (Wong, W. *et al.*, *2010*) were also analyzed in this paper. This other study (hereafter referred to as the "previous study") used the same instruments and tests. The previous study, however, released both gases simultaneously after allowing the MIRAN SapphIRe to collect data for two minutes. All tests for the previous study were performed with the sash height raised to 710 mm. Analysis of the data from these tests began one minute after the gas was turned on as well. Only four minutes of the data was analyzed, however, due to differences in test conditions after this point. Because the previous study used two dispensers inside the hood simultaneously, neither could be centered directly in front of the mannequin as specified by ASHRAE 110. The current study used only one dispenser at a time, and it was centered in front of the mannequin as specified by ASHRAE 110.

Data Desk (Data Description Inc., Ithaca, N.Y.) was used for linear regression and to determine averages, standard deviations, and other descriptive statistics.

Computations for Time Lag due to dilution in the instrument chamber

Assuming that the sampled concentration was constant after the gas was turned on, the time for the apparatus's recorded measurements to approach their actual values can be approximated using the well-known single-cell mass balance model (Committee on Industrial Ventilation, 1998), which can be integrated to produce:

$$C_t = C_{t1}e^{-Q\Delta t/mV} + (C_s + \frac{Gm}{Q})(1 - e^{-Q\Delta t/mV}) \dots\dots\dots\dots\dots(1.6)$$

C_t = instantaneous concentration of specified gas observed by MIRA

C_{t1} = initial concentration of gas

C_s = concentration entering the MIRAN from probe

Q = exhaust rate, m = mixing factor

V = volume of MIRAN chamber

G = generation rate

Q/m = decay rate

In this setting, the initial concentration of as, C_{t1}, and generation rate, G, are 0. The exhaust rate, Q, and volume of the MIRAN chamber, V, can be determined from the manufacturer's specifications. They are found to be V = 2.23 liters and Q = 15 LPM. Maughan *et al.* (2005) determined the time to 90% of steady-state input concentration for the MIRAN SapphIRe. The investigator for this study substituted this value of time into the dilution equation (Equation 1.6) to calculate the corresponding value of the mixing factor, m. This value was found to be m=2. The mixing factor is determined by the mechanical properties specific to the machine will be nearly identical for each instrument of the same model. The value of the mixing factor was applied to determine a time of 42 seconds to reach 90% of the actual input value for the current study. This means that any data collected before 42 seconds after the gas has been turned on will be less than 90% of the steady-state input value. For that reason, initial data has been excluded from this report. All data collected after this point of time up until the five minute end point has been included. This includes concentration values outside of the range of accuracy specified by the manufacturer.

Omitting the initial data violates ASHRAE 100 specifications but the purpose here is to compare the behavior of SF_6 and N_2O, not to rate the hoods per se.

RESULTS

The results for the velocity measurements, smoke tests, and tracer gas tests are discussed below. The results are based on analyses of two sets of data collected. The "Previous Study" data was collected previously by other researchers using the same apparatus and methods as were used in the current study ("Current Study" data). The most substantial difference was that in the Previous Study the N_2O and SF_6 were released separately but concurrently from two different identical diffusers placed adjacent to each other when testing each hood. In the current study, each hood was tested with SF_6 released from one diffuser placed in the center of the hood followed immediately by a test with N_2O released from the same diffuser in the same location.

As will be shown, the difference in results for N_2O and SF_6 from the previous study showed substantially less variability than the current study, perhaps because SF_6 and N_2O were released and sampled simultaneously rather than 10-15 minutes apart.

Velocity Measurements

Face velocity measurements were taken at many points for each hood. Large fluctuations were observed between measurements at each location for the same hood. This was likely due to both uneven flow into the hood and asymmetry of the internal configuration. Additionally, minute differences in anemometer positioning, especially in aligning the instrument with the plane of the sash may have contributed to the large variations resulted in significant changes in readings. There were noticeable differences in average face velocities between hoods, but they were less than the differences between individual measurements of the same hood. The mean, median, standard deviation, minimum, maximum, and middle values were determined for each hood. The full list of values can be seen in Appendix I. Table 4 contains a summary of the averages of each statistic. The face velocity measurements of the previous study were generally lower and had less variability than the measurements of this study.

Table 4: Face Velocity Summary

	Mean (m/s)	Median (m/s)	Standard Dev (m/s)	Min (m/s)	Max (m/s)
This Study	0.328	0.323	0.0528	0.251	0.410
Previous Study	0.272	0.261	0.0335	0.228	0.351

Smoke Observations

The smoke test results were determined on a pass-fail basis. To pass, a hood must sufficiently contain the gas along every point around the perimeter. Results were used to verify the functionality of each hood and were not used for any further analysis. Every hood tested in this study received a passing score.
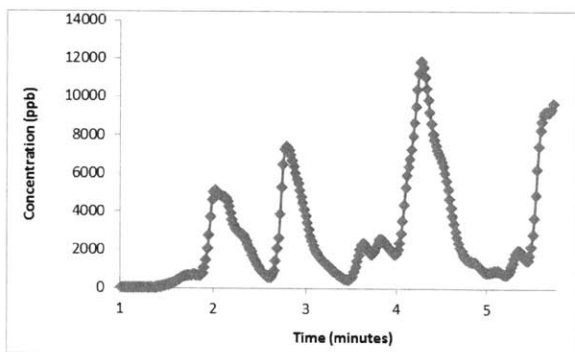
Figure 6: SF$_6$ Concentration (Hood: 8-101-1)
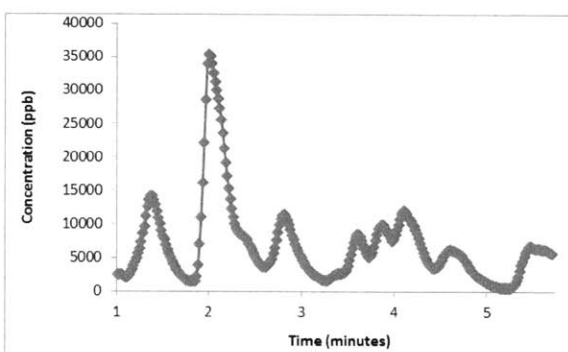
Figure 7: N$_2$O Concentration (Hood: 8-101-1)

Tracer Gas Test Results for SF$_6$ and N$_2$O

Figures 6 and 7 each show time-series data for the full-open condition of a hood for SF$_6$ and N$_2$O, respectively. As was common in hoods with high leakage, there are numerous peaks and troughs in both graphs. The magnitude and time delay between peaks showed no apparent repeating pattern for any given hood. Peaks with less leakage typically had one large peak or none at all. Despite having roughly the same delay between gas being turned on and the first datum included in the analysis, the time to the first peak varied greatly and without an apparent relationship to the overall amount of leakage. Figure 7 reaches its first peak around 1:20 after data logging began, whereas Figure 6 doesn't reach it until around 2:00. This large difference could be due to changing temperature gradients and to changing room airflow conditions due to ebbs and flows in the supply and exhaust of air. Overall, the time-based results generally show high variations in both SF$_6$ and N$_2$O levels over time and between different hoods.

Time Lag Until Representative Sampling

For roughly 1 minute (not shown) the concentrations were very low because the MIRAN SapphIRe is turned on before the tracer gas begins to flow (see Procedure). During this period the gas is turned on, the tracer gas fills the hood, and the sampled air mixes with the uncontaminated 2.3 L of air in the sampling chamber. After one minute, the sampled air has largely replaced the uncontaminated air and the concentration often rises sharply. The first minute is not representative of the hood performance and is omitted from quantitative analyses.

The sampling chamber functions as a 2.3 L mixing chamber with a sample rate of roughly 15 LPM. The time to complete mixing is roughly 42 seconds (see Tracer Measurement Instrument). The reported concentration at any point in time is strongly affected by the previous 42 seconds of sampling. This results in patterns that appear smoother than they are in reality. As shown in Figures 6 and 7, many plots had exponential declines after peaks that took around 42 seconds to reach the trough. This indicates the presence of a few very high concentrations appearing briefly and then disappearing. The 42 second exponential decline reflects the time it takes the sampling chamber to flush out the brief, high concentration. Time-based outputs were very chaotic and unpredictable. The actual levels of each gas present were likely even more extreme due to the averaging effect of the instrument's data processing method.

Analysis of time based results is a poor indicator of containment ability due to the difference between measured and actual conditions inside the hood. Overall concentration

averages for each test were used to better model behavior. Due to the large peak contribution, however, one would expect to see high variability of the average in repeated testing.

Observed Concentration Ranges and the Accuracy Range of the MIRAN SapphIRe

The accuracy of the sampling results requires careful consideration. The MIRAN SapphIRe's accuracy in measuring SF_6 is rated by the manufacturer to within ±20% for values up to 4000 ppb. Beyond 4000, measurement values are almost certainly much less accurate. N_2O is rated within ±10% for values between 200 and 100,000 ppb. The average value of the SF_6 data in Figure 6 is 3268. This value is within the ±20% range; however, as seen in the graph, there are many individual readings that were used to compute that average that were well above the 4000 ppb threshold, thus making the average less accurate than the level of the average would suggest. Many of the SF_6 tracer gas tests in this paper had individual values above the accuracy threshold, regardless of the level of the overall average.

The number of tests with overall average concentration values within the manufacturer's specified range of accuracy was determined. No hoods had average values within this range when the sash height was in the working position. The results of the full open portion of this study and the previous study were plotted in Figure 8; they were plotted as logs so that every individual point can be seen on one chart. 31% of N_2O measurements and 62% of SF_6 measurements for these conditions were within the range. The results of 24% of these tests had measurements for both gases in the range of accuracy as illustrated by the green rectangle in Figure 8. This means only 24% of all correlations can be said to be accurate if only the accuracy of average values are used. In reality, many more tests with average values within the range had individual measurements outside. As a result, the accuracy of all results cannot be known. Due to the instrument's calibration techniques, values outside the range are likely underestimates.

The effect of the chamber's dilution-averaging necessarily obscures the true peaks at the probe inlet. For example, as can be shown with Equation 1.6 a step increase to 4000 ppb that continues for 10 s then instantaneous declines to zero would achieve a peak of roughly 1700 ppb at the end of 10 s and roughly 600 ppb 10 s later. Hence, average concentrations in hoods with high leakage can be dominated by very short duration spikes of leakage.

The instrument sensor "sees" the concentration throughout the chamber, not at just the inlet, so the true peaks are not relevant to accuracy issues because the instrument measures light absorption for the chamber as a whole rather than at the inlet.
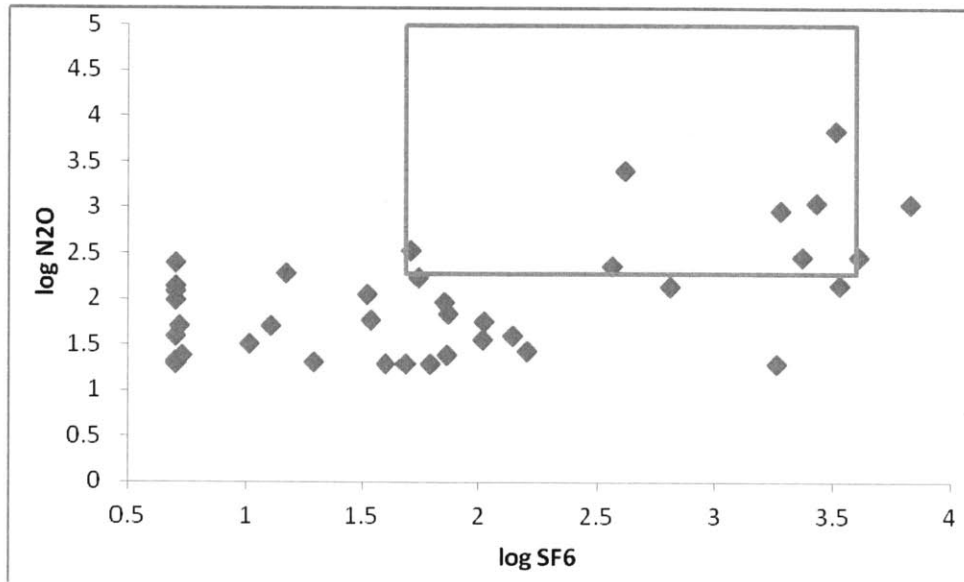
Figure 8: Range of Accuracy of Results
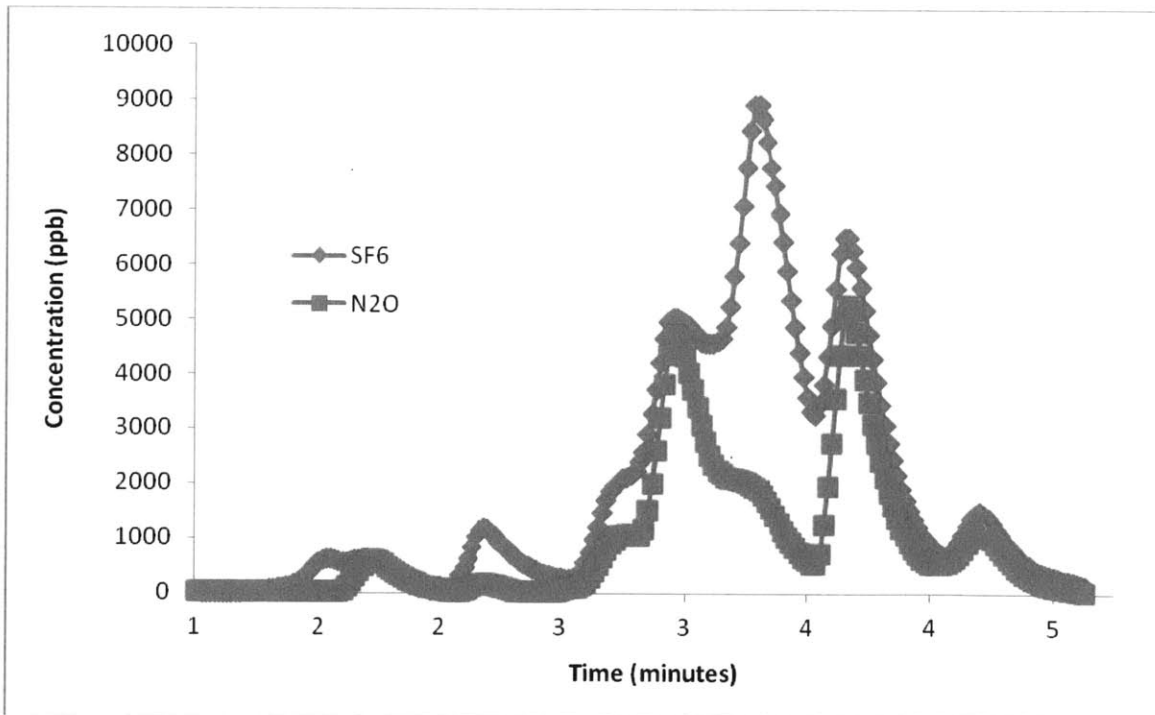
Figure 9: Typical Concentration Over Time for Previous Study
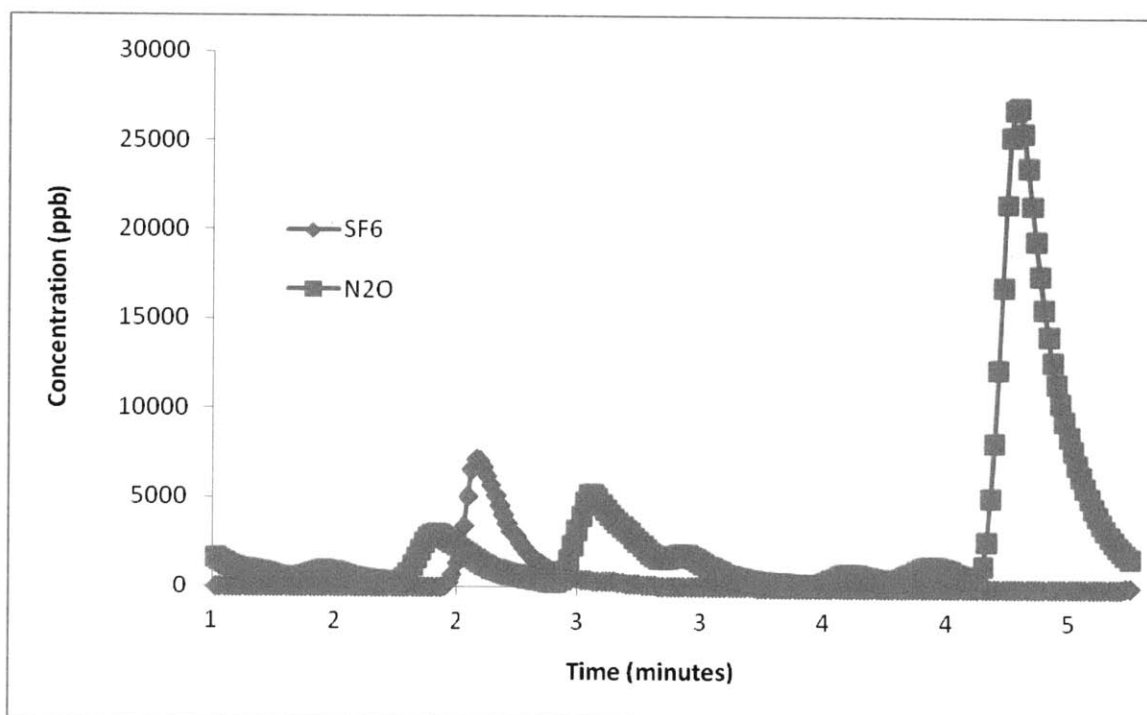
Figure 10: Typical Concentration Over Time for This Study

Effects of concurrent and non-current release of N₂O and SF₆

In the previous study, both gases were released simultaneously; in this study, they were released at separate times. Conditions inside the hood vary randomly over time. The five minute average is a random sampling of hood conditions. Releasing the gases at the same time means they will experience a more similar environment. It may potentially reduce some variability in the results compared to the current study.

Tests with high leakage often had multiple peaks, while those with less leakage typically had one or no peaks. Tests with both gases released simultaneously had an increased chance of having their peaks occurring at the same points in time. An example of a hood with multiple peaks occurring at the same points in time can be seen in Figure 9. Unaligned peaks present in another hood's results are in Figure 10. Figure 10 shows both low leakage of SF₆ with a single peak and high leakage of N₂O with multiple peaks. Tests with one gas leaking substantially more than the other were common.

The level of reduction in variance attributed to the simultaneous release of gas likely varies with leakage levels. The presence of a few peaks largely determines the average concentration of the test. In tests with low levels, peaks occur less frequently, often once or never. When they do occur, however, they often increase the average by orders of magnitude. It is likely that for a given hood, repeated testing would show that these peaks occur more frequently in some 5 minute periods than others. If so, the test results for a hood could vary randomly over a broad range. Since hoods, in practice, are each tested only for one 5-minute period, the number of peaks recorded could be a matter of chance rather than the consequence of controllable conditions near the hood. When both gases are recorded separately, they are less likely to report the same number of peaks. The difference in the number of peaks observed based on the

period of time analyzed likely affects the results of tests with low leakage more due to their small number of peaks. Consequently, the difference in results between concurrent and non-current release of N_2O and SF_6 is expected to be higher in tests with lower average concentrations.
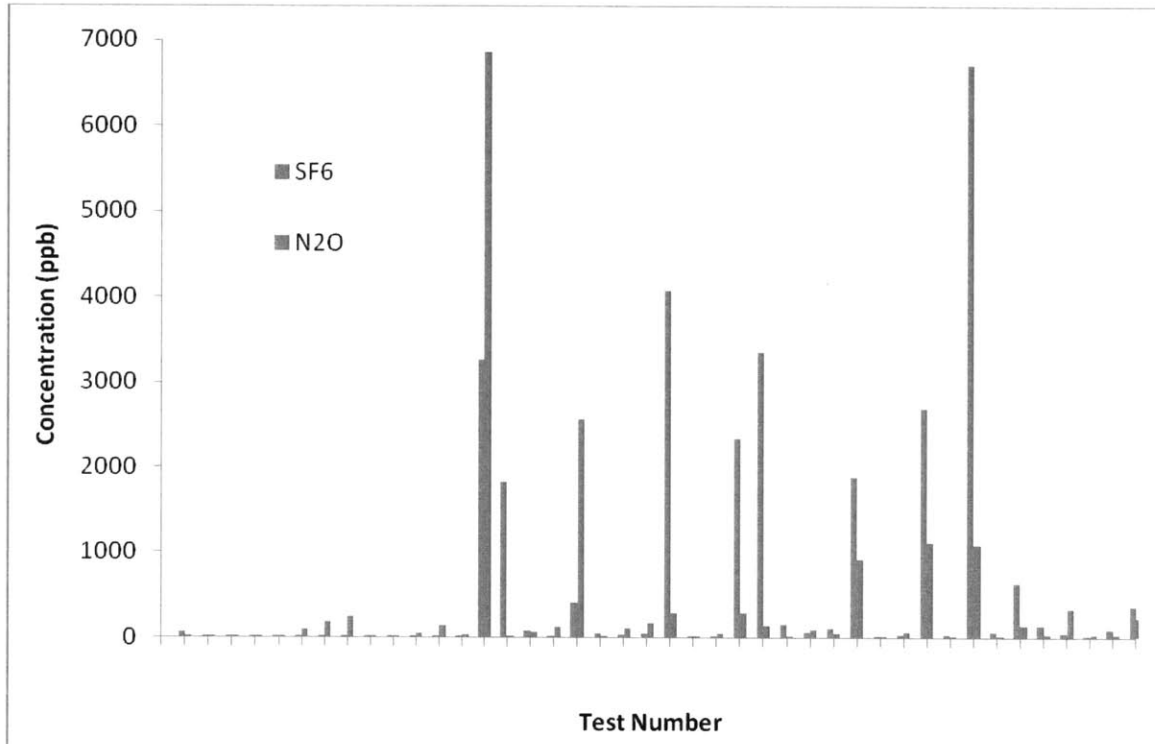
Figure 11: Concentrations for Each Test Condition

Table 5: Statistics for Each Test Condition

Condition	SF_6 Mean	SF_6 Median	SF_6 Std Dev	N_2O Mean	N_2O Median	N_2O Std Dev
This study working height	10.8	5	15.9	69.8	21.3	76.9
This study full open	1196	75.5	1558	827	121	1941
Previous study	820	105	1750	267	58.8	399

Five minute averages of time based concentration data are the source of data used most for analysis in this paper. This is in accordance with the ASHRAE 110 method. Figure 11 shows the concentrations for both gases for each setup configuration. A unique test number was assigned for each sash position at every hood to distinguish between tests. This number is solely used to neatly display the results of large numbers of tests. The corresponding condition and numerical results for each test condition can be seen in Appendix I.

Table 6: Effect of Sum of Highest Concentrations on Overall Sum for Full Open, Working Height, and All Sash Positions

	SF$_6$ Sum >500ppb	SF$_6$ Total	%	N$_2$O Sum >500ppb	N$_2$O Total	%	Sash Position
This study	14891	15687	95%	9436	11656	81%	All
Previous study	11964	13122	91%	3147	4271	74%	All
This study	14891	15547	96%	9436	10748	88%	Full
This study	0	140	0	0	908	0	Working

Effect of Excursions on 5-minute Time-Weighted Averages

For the time series data, "outliers" played a large role in determining five minute averages. The mean values shown in Table 5 and Figure 11 are strongly dependent on the highest observed values. Table 6 shows the summation of every average concentration above 500 and compares it to the total. As seen in the table, values above 500 almost entirely determine the overall results. The outliers come exclusively from the full open condition. As seen in Table 6, there are no values for either gas above 500 when the sash is set at the working height. Essentially, very high values from the full open condition are making the results of the working sash height configuration irrelevant when compared together. As a result, later analysis separates the results of the two conditions.

SF$_6$ and N$_2$O Concentrations

As seen in Figure 11 and Table 5, there were enormous differences in the results of 5 minute averages between different hoods and for the two gases. As shown in Table 5, as would be expected, the average and median concentrations determined when the sash was in the low, "working" level were small fractions (i.e., roughly 10%) of the concentrations when the sash was fully open. Even more striking was the very high standard deviations and the great disparity between the mean and median values for both gases and both datasets across all hoods tested. The high standard deviations and the differences between means and medians both suggest a highly asymmetric, highly non-normal distribution of concentrations of both gases among the hoods.

Table 7: Amount of Tracer Gas Outside Specified Values for Ratios of SF_6 to N_2O

Source of Data	Sash Opening	Hoods Tested	SF_6, N_2O both < LOD	Threshold Ratio	No. SF_6/N_2O > Ratio	No. N_2O/SF_6 > Ratio	Sum ppb SF_6 outside Range	Sum ppb N_2O outside Range	Sum ppb All SF_6	Sum ppb All N_2O	% SF_6, N_2O both < LOD	N_2O/SF_6 >Ratio %	SF_6/N_2O >Ratio %	Ratio >Thresh %SF_6	Ratio >Thresh %N_2O
Current	Full	13	0	1.5	6	5	15453	10659	15547	10748	0%	46%	38%	99%	99%
Previous	Full	16	1	1.5	3	11	13045	4153	13122	4271	6%	19%	69%	99%	97%
Current	Partial	13	7	1.5	5	1	105	747	140	908	54%	38%	8%	75%	82%
Current	Full	13	0	3	5	4	12136	3762	15547	10748	0%	38%	31%	78%	35%
Previous	Full	16	1	3	2	4	7723	1673	13122	4271	6%	13%	25%	59%	39%
Current	Partial	13	7	3	5	1	105	747	140	908	54%	38%	8%	75%	82%
Current	Full	13	0	6	3	4	12047	3476	15547	10748	0%	23%	31%	77%	32%
Previous	Full	16	1	6	1	1	6772	1435	13122	4271	6%	6%	6%	52%	34%
Current	Partial	13	7	6	4	0	30	677	140	908	54%	31%	0%	21%	75%
Current	Full	13	0	10	2	3	9296	622	15547	10748	0%	15%	23%	60%	6%
Previous	Full	16	1	10	0	0	0	0	13122	4271	6%	0%	0%	0%	0%
Current	Partial	13	7	10	4	0	30	677	140	908	54%	31%	0%	21%	75%
Current	Full	13	0	15	1	2	5200	282	15547	10748	0%	8%	15%	33%	3%
Previous	Full	16	1	15	0	0	0	0	13122	4271	6%	0%	0%	0%	0%
Current	Partial	13	7	15	3	0	15	483	140	908	54%	23%	0%	11%	53%
Current	Full	13	0	20	1	2	5200	282	15547	10748	0%	8%	15%	33%	3%
Previous	Full	16	1	20	0	0	0	0	13122	4271	6%	0%	0%	0%	0%
Current	Partial	13	7	20	2	0	10	385	140	908	54%	15%	0%	7%	42%

　　　　　　29

SF₆ and N₂O Concentration Comparisons

As discussed earlier, concentrations of SF_6 and N_2O each varied greatly. A comparison of the concentration of one gas to the other also produced highly variable results. N_2O concentrations were greater than SF_6 about as often SF_6 concentrations were greater than N_2O. There was very often a large ratio between SF_6 and N_2O (see Table 7). Due to the somewhat even number of cases with each gas higher, any analysis that effectively averages the ratios together would result in a relationship closer to 1:1. This aggregation would obscure the crucial fact that for specific hoods, the two gases produced substantially different results.

In order to better show the magnitude of the discrepancy between SF_6 and N_2O, the number of conditions that resulted in large ratios between the substances is shown in Table 7. A threshold ratio of 2 means that the five minute averages of SF_6 were at least twice as high as N_2O or the average of N_2O was at least twice as high as SF_6. Every test that had the average concentration of either gas equal to its detection limit was excluded to take into account the inherent difference in detection ranges. The results can be seen in Table 7. The ratio between gases was rarely close to 1. The regular occurrence of unbalanced ratios continued into high differences and also often occurred when one was below the limit of detection and the other was very high.

A few of the average concentration values are so large that they make the analysis of the rest of the points impossible. They are not the result of test mistakes, and they are likely not consistently repeatable. If every test were redone repeatedly, the highest concentration observed would likely shift between hoods regularly. Despite their randomness, they cannot be ignored due to their high occurrence and legitimacy. To make correlations incorporating all of the data, log plots were performed to reduce the impact of the driving outliers. The log plot of the combined data from both studies can be seen in Figure 12. While it has a few values noticeably larger than the rest, no outliers stick out nearly as much as on previous figures. If this were not a log plot, the five values in the top right corner of the chart would be much further away and make all other points nearly irrelevant in the calculation of the correlation. The best fit line has a slope of 0.858, a y-intercept of 0.434, standard deviation of 0.76, and an R^2 of 35.9%. This is not an especially strong correlation, especially for a log plot. The non-log plot will have nearly no correlation whatsoever.
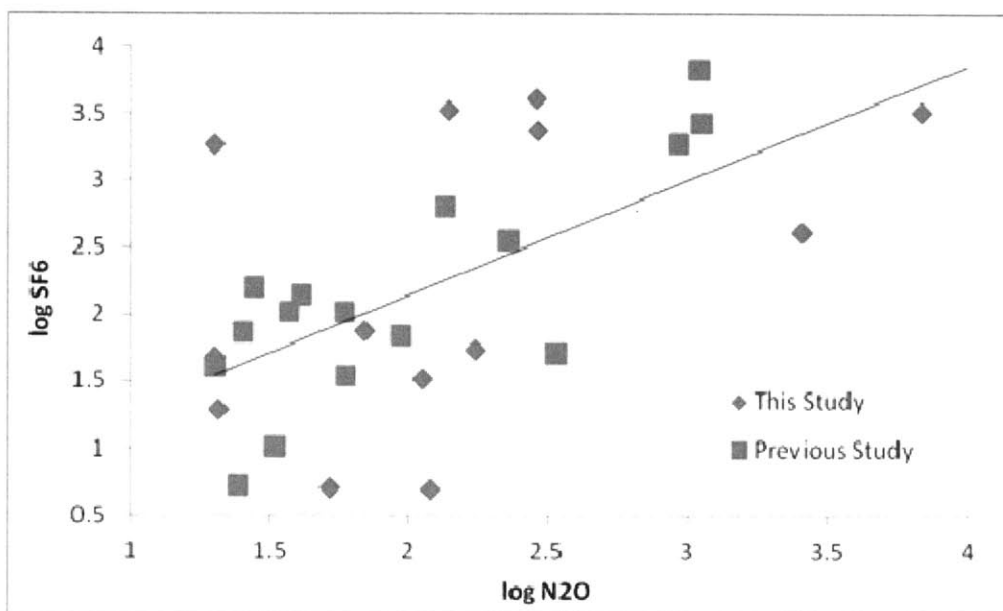
Figure 12: Log Plot for Data from Previous Study and Full Open Condition of This Study

Comparison of SF₆ to N₂O

Failure Rate for Hood Tests

The ANSI standard requires a hood maintain a 5 minute average concentration below 100 ppb to pass. The failure rates for each condition can be seen in Table 8. Failure rates were similar for conditions with high sash height; however, hoods that failed for one gas failed for the other only 67% of the time. When less leakage was observed in the working sash height position, N_2O was the only gas to pass the 100 ppb threshold. The difference in detection limit (40 ppb for N_2O and 10 ppb for SF_6) likely played a large role in this difference.

Table 8: Failure Rate of Hoods for Both Studies

Sash Position	Fraction of Hoods Failing With N_2O	Fraction of Hoods Failing With SF_6	Fraction of Hoods Failing With Both SF_6 and N_2O	Fraction of Hoods that Failed SF_6 Also Failing N_2O	Fraction of Hoods that Failed N_2O Also Failing SF_6
Working Sash Height	23%	0	0	0	0
Above Working Sash Height	48%	52%	34%	67%	67%

Effect of Sash Height

The results of other studies indicate that increases in sash height result in increased leakage with poor correlation. Sash height was examined to determine its impact on the ratio of SF_6 to N_2O. The effect of varying positions for each gas can be seen in Figures 13 and 14. Increases in

the height of the opening resulted in overall higher average concentrations for both gases. SF_6 has a $p<0.0001$ and an R^2 of 30%. This indicates that sash height and SF_6 concentrations are related, but sash height alone is only a modest predictor of behavior. This is consistent with the results of other studies. N_2O has lower values for both terms at a 5.6 value for R^2 and $p<0.07$. This suggests less of a correlation between the two variables for N_2O. Other variables account for a larger portion of the variance. This difference in responses of N_2O and SF_6 supports the conclusion that they behave differently as sash height changes. The plot of the ratio of the two gases as seen in Figure 15 provides additional evidence. The best fit line has a slope of 0.0032 with an R^2 of 21.5%. The relationship between $\log(SF_6/N_2O)$ and sash height is highly significant ($p<0.0012$). Sash height greatly affects the SF_6 to N_2O ratio present in each test in a manner difficult to predict.

Sash height's appeared correlation may only be present as a result of a relationship with the area of the opening of the hood. Other studies have shown that area affects leakage rates, and sash height contributes much more than width. To determine the roles of each factor, the statistical correlation was performed using both sash height and width as variables. An R^2 value of 30.3% was determined as well as $p<0.0017$ and $p<0.0185$ for sash height and width, respectively. Width as a factor by itself had no correlation to leakage rates. When area (height * width) was used as the variable, there was an R^2 of 27% and $p<0.0002$. This shows that the area of opening is very important in determining concentration. Area is a better indicator than sash height alone, and sash height contributes much more than width.
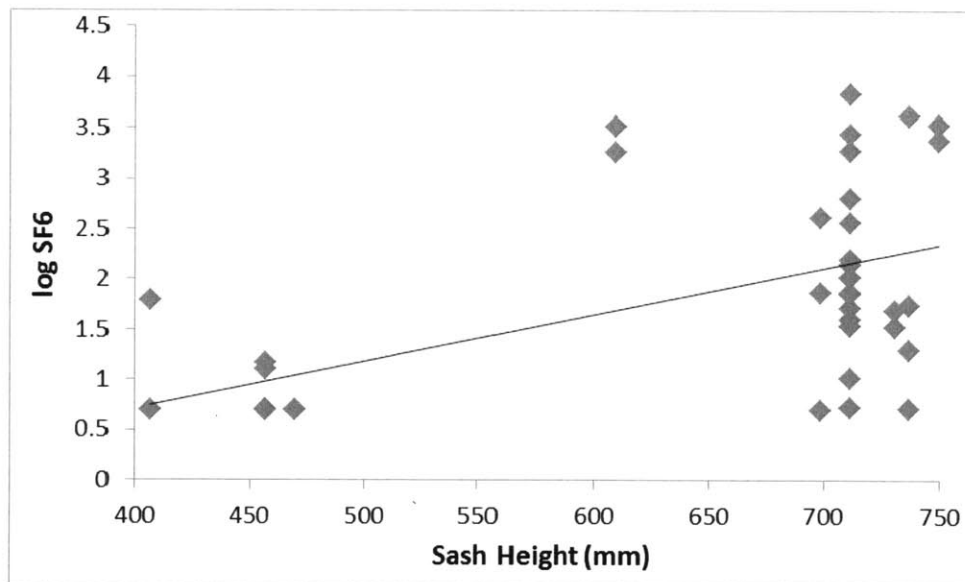
Figure 13: SF_6 Concentration Compared to Sash Position
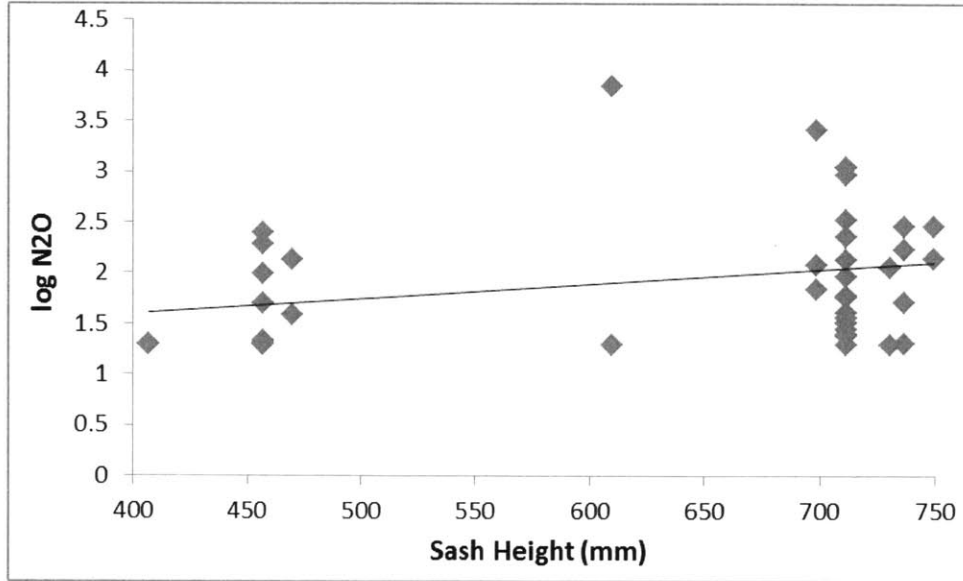
Figure 14: N_2O Concentration Compared to Sash Position
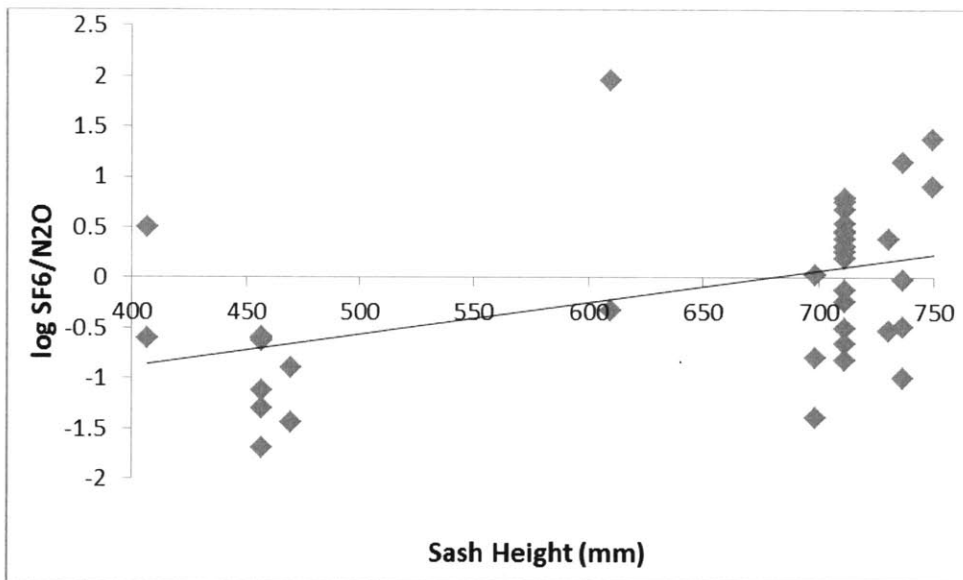
Figure 15: SF_6/N_2O Ratio Compared to Sash Position

Effect of Face Velocity

The designs of the hoods examined in this paper depend heavily on face velocity for containment. SF_6 and N_2O may potentially behave differently with changes in velocity. To qualify as a valid substitute, N_2O must behave predictably in relation to SF_6 during all conditions reasonably expected for a fume hood. Potentially as velocity increases, the log of the ratio may go to 0 if concentrations become closer. Velocity measurements varied greatly between the different grid locations of each hood. The deviations due to location are probably strongly affected by changes in seemingly minor minute-to-minute airflow patterns in the room. The

summary of all measurements can be seen in Table 4. The minimum, maximum, and standard deviation of velocity readings at each hood were found to have a much lower correlation with its concentration values than the average and middle grid values. The relationship between average and middle velocity and SF_6 to N_2O ratio for this study can be seen in Figures 16 and 17. The R^2 of the average velocity figure was 32.2%, and $p<0.025$. The R^2 of the middle velocity figure was 33.9% and $p<0.0216$. Both of these relationships have higher R^2 and P-values than sash height. The higher R^2 observed indicates that face velocity is a better indicator of the SF_6 to N_2O ratio. The middle velocity measurement was a slightly better predictor than the average. Both sets of values were very similar, but it was expected to follow this behavior. The gas would be expected to correlate best with the face velocity observed in the position it was released. The face velocity measurements from the previous study had no relationship with any concentrations and were excluded. This is potentially due to differences in measurement technique.
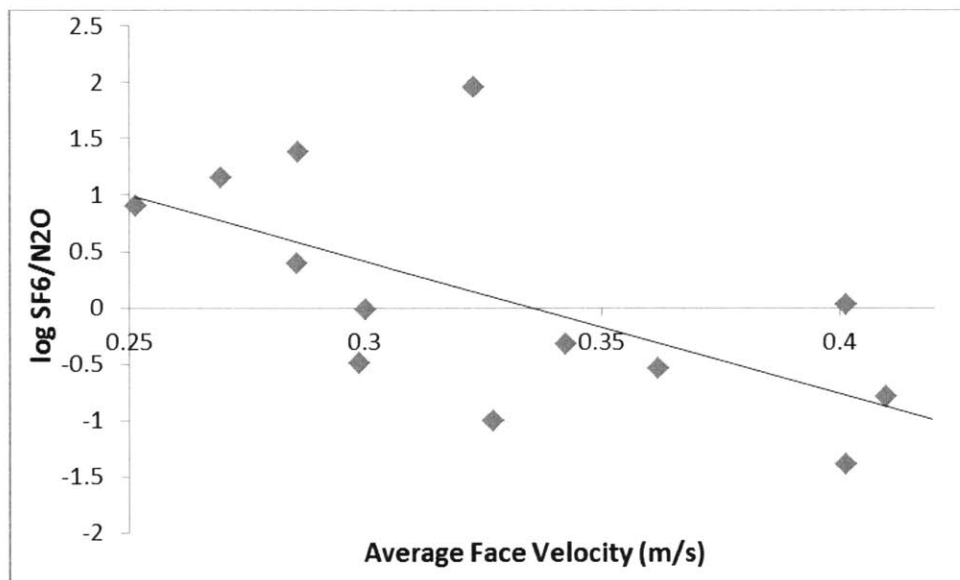

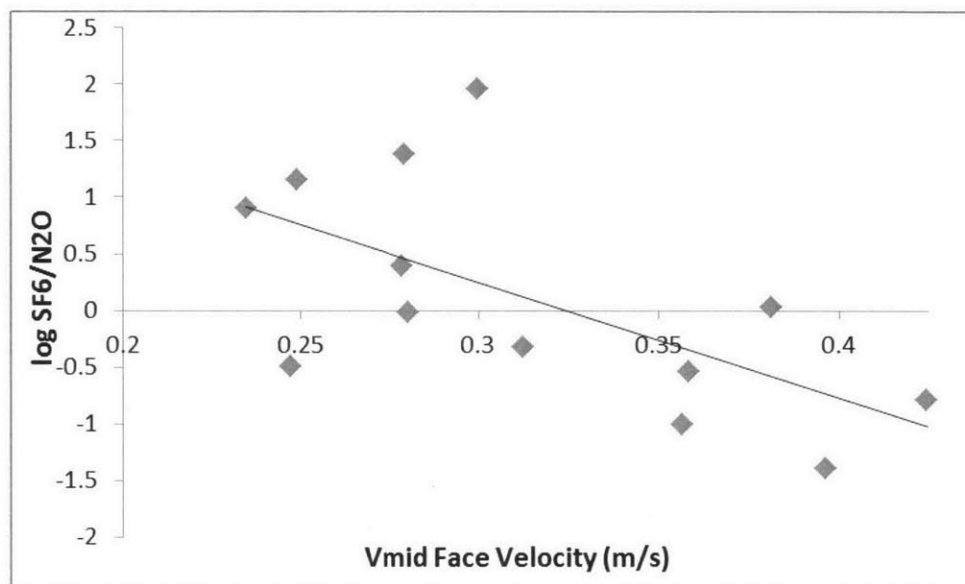Figure 16: Average Face Velocity Compared to SF_6/N_2O for This Study

Figure 17: Middle Face Velocity Compared to SF_6/N_2O for This Study

DISCUSSION

The most important characteristic of a gas for use in testing hoods is its ability to predict the behavior of contaminants potentially used in each hood. SF_6 is specifically favored for use as a tracer gas in ASHAE 110, though other tracer gases are acceptable if they are shown to produce similar results.

Accuracy of measurements was hindered by MIRAN SapphIRe limitations and requirements in ASHRAE 110. The MIRAN SapphIRe's mixing chamber obscures time-series results due to time-averaging. Given that 42s is required to achieve 90% of a steady-state input value, the actual inputs are likely to be far more chaotic than the time-series graphs (see Figures 6 and 7) portray. The ASHRAE 110 guidelines limit the data logging to 5 minutes instead of a much longer duration which likely results in increased variability of test results for the same hood taken at different times.

For N_2O to serve as a substitute, it must behave predictably in relation to SF_6. While ideally they would behave identically, a consistent correlation of sufficient strength may be enough. The correlation should be robust in the face of the wide range in hood designs, face dimensions, and room conditions that affect hood test results when SF_6 is employed. The results for both the Previous Study and the Current study both showed negligible correlations when N_2O and SF_6 were compared without log-transformations.

Because of the extreme ranges and skewed distributions of both SF_6 and N_2O, all analyses were done using $\log_{10}(SF_6)$, $\log_{10}(N_2O)$, and $\log_{10}(SF_6/N_2O)$. Since $\log_{10}(SF_6/N_2O) = \log_{10}(SF_6) - \log_{10}(N_2O)$, its use avoids the problems normally associated with analyses of ratios.

The factors governing fluid dynamic behavior in the laboratory fume hood are enormously complex and are largely affected by randomness. Accuracy of measurements was hindered by MIRAN SapphIRe limitations. Leakage rates for individual tests were chaotic and unpredictable. Even the five minute average results of these tests were extremely varied. Wide margins that fluctuated significantly in magnitude were observed in the ratios of average SF_6 and N_2O concentrations. Each gas leaked orders of magnitude higher than the other at similar levels of occurrence. As a result, the correlation between the two gases was weak.

Sash height and area of sash opening both significantly ($p<0.001$) affected $\log_{10}(SF_6/N_2O)$, but the overlap in results with different levels was very high, which is consistent with the findings of Ahn *et al.* (2008). Hence, one cannot predict SF_6 using N_2O with reasonable precision using hood dimensions.

Average face velocity significantly ($p<0.025$) affected the log-ratio for the current data and produced an $R^2= 0.32$. For the previous study data, the relationship was essentially random ($R^2= 0.02$). Substituting for the average with the median, middle location, and standard deviation did not produce a better fit. Likewise, Maupin and Hitchings (1998) were unable to create a consistent model for predicting contaminants using mean velocity, velocity profile, and turbulence measurements. They said, "This does not mean that there is no correlation, but that no adequate model has yet been devised to predict containment without actually measuring it." The low correlations of the variables in this study indicate that other unaccounted factors are playing a strong role.

Independently, both the weak correlation between SF_6 and N_2O concentrations and the influence of hood specific traits each suggest N_2O is a poor substitute. Together, they provide

36

substantial evidence for this conclusion. This does not necessarily mean that N_2O is worse at predicting contaminant behavior than SF_6. There is no way to judge which tracer gas better mimics lab contaminant behavior in hoods during work.

The wide variations of leakage rates in hoods that typically had only minor differences suggest that the test method could be highly sensitive to minor variations in room conditions, such as local cross-drafts due to diffusers and returns. Since airflows to the room often vary widely over time, a test result found at one time could have little correspondence to results taken at any other point in time. If so, the test would offer poor specificity when applied to individual hoods. It is possible that the radical differences in N_2O and SF_6 results taken a few minutes apart may be a consequence of random differences with time as opposed to differences between the two gases. Results were found to sometimes vary sharply even when all conditions and hoods appeared to be the same. This suggests a level of sensitivity to minor changes so extreme that the results of these tests might be meaningless.

The tracer gas test as described in the ASHRAE 110 method may not be a good indicator of hood containment performance. Tseng *et al.* (2006) found significant differences in leakage at varying locations at the hood face. The breathing zone was shown to leak substantially less than other locations, and this study only tested the breathing zone. Tracer gas tests using unheated mannequins have been shown to be unrepresentative of human usage of hoods (Gao and Niu, 2005; Ahn *et al.*, 2008). Heat generated from the human body greatly alters the dynamics of contaminants. Finally, it is conceivable that movement from hood users during normal work may noticeably change exposure levels. (Ahn *et al.*, 2008)

For future research, I would recommend a much longer testing period and repeated testing at each hood. Repeated testing would help identify how much of the variation between gas concentration ratios was due to the randomness of hood performance. Longer test periods would likely decrease the variance in results between repeated tests at the same hood by reducing the contribution of individual concentration peaks. Additionally, releasing a mixture of both SF_6 and N_2O from a single dispenser may yield results more relevant to evaluating SF_6 as a replacement for N_2O. Finally, it would be worthwhile for future research to explore the repeatability of the ASHRAE 110 test itself. If the test is found to be unable to repeatedly rank the effectiveness of hoods, then the procedure should be corrected or replaced.

CONCLUSIONS

The overall conclusion of this study is that N_2O and SF_6 do not give comparable results when testing hoods using the modified version of the ANSI/ASHRAE 110 standardized test of hood containment performance employed here. The specific conclusions of this study are:

1. Concentration measurements logged by the MIRAN SapphIRe are strongly influenced by conditions sampled at the probe within the previous 42 seconds.

2. Peak concentrations of the concentrations at the probe are obscured by the running average of mixing in the chamber.

3. It is likely that the bulk of exposures to the mannequin came in short, highly concentrated spikes. Hence, the overall average concentration for each hood is largely determined by the values of a few peaks.

4. The upper limit of the manufacturer's claimed range of accurate readings was often substantially exceeded.

5. The reported concentrations were often at or below the limit of detection, complicating comparison of ratios of N_2O to SF_6.

6. Concentrations of both gases were highly variable and didn't follow a normal distribution.

7. Nearly all of the total exposure came from a few of the tests with the highest average concentration.

8. When the sash was above the working height, both SF_6 and N_2O exceeded the 100 ppb failure threshold at about the same rates. When the sash was set at the working height, only N_2O ever reached 100 ppb.

9. When a hood exceeded the 100 ppb failure threshold for one gas, it only had a 67% chance of failure for the other gas.

10. The log of the gas concentrations improved the linearity of the relationship between N_2O and SF_6 but between the effects of the modest R^2 and the effects of log-transformation for regression analyses, the anti-logs of the prediction model had negligible utility for predictions.

11. The log-ratio of the two gases varied depending on sash height, area of opening, and face velocity, indicating the gases behave differently under different conditions. This strongly supports the general conclusion that N_2O and SF_6 cannot be usefully substituted for each other.

12. It is possible that the differences in results for N_2O and SF_6 are due to their differences in density

13. An unknown but probably substantial portion of the variations in results for different hoods was due to temporal variability. That is, the same hood tested multiple times may well have a variance in results similar to the variance of different hoods tested at different times

WORKS CITED

1. **Ahn, K., S. Woskie, L. DiBerardinis, and M. Ellenbecker:** A Review of Published Quantitative Experimental Studies on Factors Affecting Laboratory Fume Hood Performance. *Journal of Occupational and Environmental Hygiene.* 5: 11, 735-753 (2008).

2. ANSI/ASHRAE 110-1995. "Method of Testing Performance of Laboratory Fume Hoods" (1995).

3. **Antweiler, R.C. and H.E. Taylor:** Evaluation of Statistical Treatments of Left-Censored Environmental Data Using Coincident Uncensored Data Sets: I. Summary Statistics. *Environmental Science and Technology.* 42, 3732-3738 (2008).

4. **Caplan, K.J., and G.W. Knutson:** A Performance Test for Laboratory Fume Hoods. *American Industrial Hygiene Association Journal. 43,*722-737 (1982).

5. CMB Control. "MIRAN SapphIRe Series Analyzers for Monitoring Toxic Substances in Fume Hoods." (2010) http://cmbcontrol.com.mx/pdf/toxic_saphire.pdf

6. **Committee on Industrial Ventilation:** Industrial Ventilation - A Manual of Recommended Practice 23rd Edition. *American Conference of Governmental Industrial Hygienists.* (1998)

7. **Gao J. and L. Niu:** CFD Study of the Thermal Environment around a Human Body: A Review. *Indoor and Built Environment.* 14:1, 5-16 (2005).

8. Intergovernmental Panel on Climate Change. "Direct Global Warming Potentials" (2007). http://www.ipcc.ch/publications_and_data/ar4/wg1/en/ch2s2-10-2.html

9. **Karaismail, Ertan and Ismail Celik:** On the Inconsistencies Related to Prediction of Flow into an Enclosing Hood Obstructed by a Worker. *Journal of Occupational and Environmental Hygiene.* 7:6, 315-325 (2010).

10. **Li, J., I. Yavuz, I. Celik, and S. Guffey:** A Numerical Study of Worker Exposure to a Gaseous Contaminant: Variations on Body Shape and Scalar Transport Model. *Journal of Occupational and Environmental Hygiene.* 2:6, 323-334 (2005).

11. **Li, J., I. Yavuz, I. Celik, and S. Guffey:** Predicting Worker Exposure – The Effect of Ventilation Velocity, Free-Stream Turbulence and Thermal Condition. *Journal of Occupational and Environmental Hygiene.* 4:11, 864-874 (2007).

12. **Maughan A.D., J.A. Glissmeyer, and J.C. Birnbaum:** Performance Evaluation of Industrial Hygiene Air Monitoring Sensors, Revision 1. PNNL-14967 Rev. 1, Pacific Northwest National Laboratory (2005).

13. **Maupins, K., and D.T. Hitchings:** Reducing employee exposure potential using the ANSI/ASHRAE 110 method of testing performance of laboratory fume hoods as a diagnostic tool. *American Industrial Hygiene Association Journal.* 59:133–138 (1998).

14. Thermo Environmental Instruments. "Miran SapphIRe." (2010) http://www.nevco.co.in/product/ambient/miran.pdf

15. ThermoFisher Scientific. "MIRAN SapphIRe Gas Analyzers for Anesthetic Agent Detection." (2010) http://www.thermofisher.com.au/Uploads/file/Miran-Anesthetic-Note.pdf

16. **Tseng, L.-C., R.F. Huang, C.-C. Chen, and C.-P. Chang:** Correlation between airflow patterns and performance of a laboratory fume hood. *Journal of Occupational and Environmental Hygiene.* 3:694–706 (2006).

17. **Wong, W., E. Zuniga, P. Greenley, and L. Norford:** Tracer Gas Substitute UROP Report. (2010)

APPENDIX I: MEAN SAMPLE VALUES FOR ALL HOODS

Table 1: Current Study, All Hood Tracer Gas Results

HoodNo	HoodID	SashHeight cm	SF_6 ppb	N_2O ppb	$Log(SF_6)$	$log(N_2O)$	$log(SF_6/N_2O)$
1	76-287	73	48.9	20.0	1.690	1.301	0.389
2	76-291	73	33.2	113.0	1.522	2.053	-0.531
3	76-311	74.9	2337.1	293.8	3.369	2.468	0.901
4	76-317	74.9	3363.2	140.8	3.527	2.149	1.378
5	76-221B_1a	73.7	55.5	173.4	1.744	2.239	-0.495
6	76-221B_2a	73.7	4090.4	289.2	3.612	2.461	1.151
7	76-391_1	73.7	19.6	20.6	1.293	1.313	-0.020
8	76-391_2	73.7	5.1	51.4	0.711	1.711	-1.000
9	5-017	69.9	74.5	69.1	1.872	1.840	0.032
10	5-022	69.9	5.0	120.8	0.699	2.082	-1.383
11	5-034	69.9	414.2	2559.9	2.617	3.408	-0.791
12	8-101-1	61	3268.1	6876.4	3.514	3.837	-0.323
13	8-101-2	61	1831.9	20.0	3.263	1.301	1.962
14	76-287	45.7	5.0	20.0	0.699	1.301	-0.602
15	76-291	45.7	5.0	21.3	0.699	1.329	-0.630
16	76-311	45.7	5.0	20.0	0.699	1.301	-0.602
17	76-317	45.7	5.0	98.4	0.699	1.993	-1.294
18	76-221B_1a	45.7	14.8	193.6	1.171	2.287	-1.116
19	76-221B_2a	45.7	5.0	248.4	0.699	2.395	-1.696
20	76-391_1	45.7	5.0	20.2	0.699	1.305	-0.606
21	76-391_2	45.7	5.0	20.0	0.699	1.301	-0.602
22	5-017	45.7	12.8	50.2	1.106	1.700	-0.594
23	5-022	47	5.0	136.4	0.699	2.135	-1.436
24	5-034	47	5.0	39.2	0.699	1.593	-0.894
25	8-101-1	40.6	62.5	20.0	1.796	1.301	0.495
26	8-101-2	40.6	5.0	20.0	0.699	1.301	-0.602

Table 2: Previous Study, All Hood Tracer Gas Results

HoodNo	HoodID	SashHeight cm	SF_6 ppb	N_2O ppb	$Log(SF_6)$	$log(N_2O)$	$log(SF_6/N_2O)$
27	143-1	71	158.9	27.7	2.201	1.442	0.759
28	143-3	71	71.2	94.0	1.852	1.973	-0.121
29	143-4	71	105.3	58.3	2.022	1.765	0.257
30	143-5	71	1894.2	929.5	3.277	2.968	0.309
31	144-1	71	5.3	24.0	0.726	1.380	-0.653
32	144-2	71	34.7	59.3	1.540	1.773	-0.233
33	144-3	71	2706.6	1121.0	3.432	3.050	0.383
34	144-4	71	40.3	20.0	1.605	1.301	0.304
35	144-5	71	6721.0	1096.7	3.827	3.040	0.787
36	163-1	71	73.2	25.1	1.865	1.400	0.465
37	163-2	71	641.9	136.7	2.807	2.136	0.672
38	163-3	71	139.5	40.9	2.144	1.612	0.532
39	163-4	71	51.4	338.5	1.711	2.530	-0.818
40	163-5	71	10.4	32.6	1.016	1.513	-0.497
41	163-A	71	104.1	36.8	2.017	1.566	0.451
42	163-B	71	363.7	230.2	2.561	2.362	0.199

Table 3: Face Velocity Statistics

HoodNo	HoodID	Height	Width	Area	Vmin	Vmax	Vavg	Vstd	Vmid
		cm	cm	cm^2	m/s	m/s	m/s	m/s	m/s
1	76-287	73	159	11593	0.229	0.335	0.286	0.035	0.279
2	76-291	73	159	11593	0.320	0.417	0.362	0.029	0.358
3	76-311	75	99	7423	0.208	0.340	0.251	0.037	0.235
4	76-317	75	99	7423	0.224	0.386	0.286	0.055	0.279
5	76-221B_1	74	152	11226	0.224	0.457	0.299	0.065	0.247
6	76-221B_2	74	152	11226	0.229	0.340	0.269	0.036	0.249
7	76-391_1	74	159	11694	0.213	0.361	0.300	0.043	0.280
8	76-391_2	74	159	11694	0.198	0.488	0.327	0.088	0.356
9	5-017	70	159	11089	0.376	0.432	0.401	0.018	0.381
10	5-022	70	98	6831	0.356	0.427	0.401	0.027	0.396
11	5-034	70	98	6831	0.386	0.442	0.410	0.026	0.424
12	8-101-1	61	224	13626	0.274	0.508	0.342	0.065	0.312
13	8-101-2	61	224	13626	0.117	0.528	0.323	0.121	0.300
27	143-1	71	188	13368	0.112	0.320	0.237	0.066	0.229
28	143-3	71	188	13368	0.152	0.351	0.247	0.049	0.200
29	143-4	71	188	13368	0.168	0.391	0.302	0.060	0.278
30	143-5	71	188	13368	0.198	0.340	0.254	0.039	0.225
31	144-1	71	188	13368	0.056	0.442	0.265	0.127	0.239
32	144-2	71	188	13368	0.168	0.284	0.237	0.028	0.218
33	144-3	71	188	13368	0.213	0.452	0.351	0.064	0.391
34	144-4	71	188	13368	0.203	0.340	0.265	0.034	0.261
35	144-5	71	188	13368	0.218	0.488	0.318	0.065	0.269
36	163-1	71	188	13368	0.183	0.351	0.295	0.042	0.295
37	163-2	71	188	13368	0.122	0.320	0.228	0.052	0.205
38	163-3	71	188	13368	0.188	0.305	0.256	0.034	0.262
39	163-4	71	188	13368	0.188	0.351	0.253	0.053	0.220
40	163-5	71	188	13368	0.163	0.411	0.254	0.064	0.234
41	163-A	71	188	13368	0.178	0.427	0.290	0.072	0.339
42	163-B	71	188	13368	0.183	0.432	0.295	0.068	0.259

Figure 1: Hood Failure Rates for Both Studies Visualized